

Multi-Objective Optimal Control of Autocatalytic Esterification Process Using Control Vector Parameterization (CVP) and Hybrid Strategy (HS)

Fakhrony Sholahudin Rohman^{1,2}, Dinie Muhammad¹, Iylia Idris³, Muhamad Nazri Murat¹ and Ashraf Azmi^{3*}

¹School of Chemical Engineering, Engineering Campus, Universiti Sains Malaysia, 14300 USM, Nibong Tebal, Pulau Pinang, Malaysia

²Department of Chemical Engineering, Universitas Brawijaya, Malang 65145, Indonesia

³School of Chemical Engineering, College of Engineering, Universiti Teknologi MARA, 40450 UiTM, Shah Alam, Selangor, Malaysia

ABSTRACT

The semi-batch esterification of propionic anhydride (PA) with 2-butanol (BT) in the presence of catalyst can be optimised using an optimal control strategy, which utilises the reactor temperature (TR) and feed (FR) flowrate. However, the opposing objective functions, which are maximum conversion (XM) and minimum process time (t_f) in the autocatalytic esterification process, could complicate the optimisation strategy. Simultaneous optimisation of various objectives results in a multi-objective optimal control (MOOC) problem with numerous solutions known as non-dominated (ND) points. In this paper, control vector parameterisation (CVP) and hybrid strategy (HS) are utilised to form Pareto Front (PF) for two opposite targets, which are first to increase XM and secondly to

reduce t_f . Each ND point comprises variant optimal dynamic tracks of TR and FR, which results in various targets of XM and t_f . These solutions provide numerous options for evaluating trade-offs and deciding on the most efficient operating strategy. It is found that the ND point in zone II can be selected as the trade-off of the optimal TR and FR in this study.

ARTICLE INFO

Article history:

Received: 16 October 2021

Accepted: 14 February 2022

Published: 21 September 2022

DOI: <https://doi.org/10.47836/pjst.30.4.21>

E-mail addresses:

fathkrk@yahoo.com (Fakhrony Sholahudin Rohman)

annursi@gmail.com (Dinie Muhammad)

iyliaidris@uitm.edu.my (Iylia Idris)

chnazri@usm.my (Muhamad Nazri Murat)

ashraf.azmi@uitm.edu.my (Ashraf Azmi)

* Corresponding author

Keywords: Autocatalytic esterification, multi-objective optimisation, optimal control, Pareto Front

INTRODUCTION

The flavour and scent reagents for the food industry consume ester from the esterification reaction. Esterification is also an essential mechanism in medicine and cosmetics production (Zulkeflee et al., 2021). In industrial practice, the ester is a salience product from batch processes generally utilised to generate high quality and particular products in small quantities while controlling the waste products and raw material losses (Rohman et al., 2021a). The sec-butyl propionate ester (SBP) is synthesised via a reaction involving propionic anhydride (PA) and 2-butanol (BT). The reaction is catalysed by sulphuric acid (Zaldivar et al., 1993).

The mathematical models for optimising esterification conditions can contribute to decision-makers evaluating and executing a wide range of options with fewer attempts (De et al., 2019). The advantages of mathematical modelling include quickly identifying the characteristics and behaviour of the esterification process, low operating costs compared to experimental trials, and increased effectiveness. However, the mathematical modelling of semi-batch autocatalytic esterification working under an unsteady state system requires a composition of differential equation system with technical limitations. Furthermore, the autocatalytic esterification process contains intrinsic nonlinear equations. Thus, optimal control provides the solution for the most effective operating strategy for the optimum time-varying feed rate (FR) and reactor temperature (TR), ensuring that production and efficiency are maximised (Faust et al., 2019).

Presently, the Single Objective Optimisation (SOO) problem is used to solve the specific reference on the optimal control of the esterification between PA and BT for SBP ester synthesis (Rohman et al., 2021a). However, opposing target functions, namely maximum conversion (XM) and lowest process time (t_f), exist in the esterification process optimisation, resulting in numerous compositions of optimum operating conditions. The optimal outcomes of the SOO problem cannot explain the relation between counteracting target functions and cannot give various sets of optimal profiles. Therefore, it is difficult to find a single solution that is best to meet all the targets. For this reason, the Multi-Objective Optimisation (MOO) approach is proposed. It is proven that by using a MOO approach, optimal strategy enhancement can provide a greater way of searching for performance trade-offs arising from opposing targets for the ester production. Nevertheless, the application of MOO in the SBP esterification process has not been reported elsewhere. Furthermore, Multi-Objective Optimal Control (MOOC) in autocatalytic ester production can address the optimisation study void for the SBP ester production process.

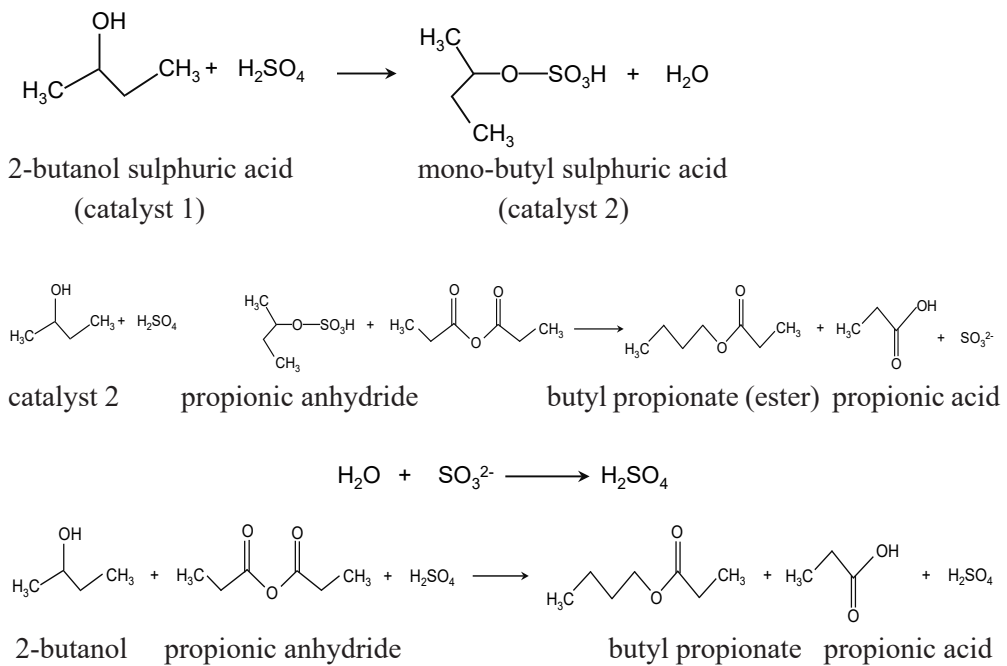
This work addresses the MOOC issue in the esterification process between BT and PA. The most effective strategy of FR and TR is determined to minimise t_f and maximise conversion, XM. Control vector parameterisation (CVP) and a hybrid strategy (HS) are utilised to execute the optimal control problem. The novelty of this research is that this

is the first time for the CVP and hybrid strategy to be applied as multi-objective optimal control of the semi-batch esterification process.

METHODOLOGY

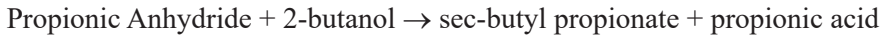
Modelling of PA and BT Autocatalytic Esterification

PA reacts with BT to yield SBP and propionic acid (PAC). The reaction occurs in a homogeneously moderate exothermic reaction. The esterification reaction is catalysed by a strong acid, such as sulphuric acid. Without the sulphuric acid catalyst, the reaction rate between propionic acid and 2-butanol is negligible in the presence of propionic anhydride. Thus, the reaction follows second-order kinetics. According to Zaldivar et al. (1993), autocatalytic behaviour occurs when a catalyst is added. He discovered that in the existence of a catalyst, the PAC increases linearly towards the reaction rate. As PAC concentration increases, the reaction rate also rises, resulting in autocatalytic behaviour. However, PAC does not influence the reaction rate once a certain concentration level is attained. Due to the complexity of the numerous theoretical autocatalytic mechanism, a model is created based on the presumption of two catalysts (cat1, cat2). The former accelerates the second-order reaction, and the latter produces a first-order reaction expression. Furthermore, the transformation of the catalysts was correlated with the acidity function and the concentration of BT. The reaction scheme for autocatalytic esterification propionic anhydride with 2-butanol used in the present reactor modelling is presented as follows:

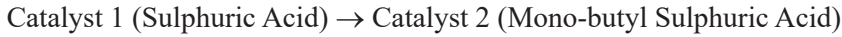


The esterification reaction mechanisms are represented as the main reaction and reaction for catalyst formation (Zaldivar et al., 1993):

Main Reaction:



Reaction for catalyst formation:



The reaction rate of the main reaction can be written as Equation 1:

$$r_1 = (k_1 + k_2 C_{cat1}) C_A C_B + k_3 C_{cat2} C_B \quad (1)$$

The reaction rate due to the formation of the second catalyst is also considered in Equation 2:

$$r_{cat} = k_4 10^{-H} C_{cat1} C_A \quad (2)$$

These assumptions considered for the construction of the model are constant responding heat capacity, reaction mixture transport characteristics, effectual overall heat transfer coefficient, and density variation exist; negligible heat losses to the environment; even distribution TR and perfect mixing: heat aggregation in the reactor wall is diminished; there are no secondary heating effects, and there is no pressure effect; BT has been designated as the limiting reactant. The acidity function expression is an empirical model which is expressed as Equation 3 (Zaldivar et al., 1993):

$$H = -(p_1 C_{cat1} + p_2 C_c) \left(p_3 + \frac{p_4}{T} \right) \quad (3)$$

Where p_{1-4} is the parameter of an acidity function.

The mass balance equations considered in the optimal control task can be assessed to denote the concentration profile in the autocatalytic esterification reaction.

The mass balances for the semi-batch autocatalytic esterification reactor are presented by Equations (4-10) as shown in Equations 4 to 10 (Ubrich, 2000):

$$\frac{dC_A}{dt} = -r_1 - \frac{F_0 C_A}{V} \quad (4)$$

$$\frac{dC_B}{dt} = -r_1 - \frac{F_0}{V} (C_{B0} - C_B) \quad (5)$$

$$\frac{dC_C}{dt} = r_1 - \frac{F_0 C_C}{V} \quad (6)$$

$$\frac{dC_D}{dt} = r_1 - \frac{F_0 C_D}{V} \quad (7)$$

$$\frac{dC_{cat1}}{dt} = -r_{cat} - \frac{F_0 C_{cat1}}{V} \quad (8)$$

$$\frac{dC_{cat2}}{dt} = r_{cat} - \frac{F_0 C_{cat2}}{V} \quad (9)$$

$$\frac{dV}{dt} = F_0 \quad (10)$$

Concentrations of BT, PA, PAc, SBP, sulphuric acid and mono-butyl sulphuric acid are denoted as C_A , C_B , C_C , C_D , C_{cat1} , and C_{cat2} , respectively. The FR, volume of solution, and TR within the reactor are denoted by F_0 , V , and T , respectively. The initial values of C_A , C_B , C_C , C_D , C_{cat1} , C_{cat2} , and V_j are 3.4M, 0M, 0M, 0M, 1.02×10^{-2} M, 0M, and 1L, respectively.

Reaction rate constants follow Arrhenius law in Equation 11:

$$k_i = k_{0i} \exp\left(\frac{E_{ai}}{RT}\right) \quad (11)$$

The reaction kinetics of this ester production have been demonstrated, and the value of kinetics information is elaborated in Table 1 from Zaldivar et al. (1993). k_1 , k_2 and k_3 are the reaction rate constant for the primary reaction. Meanwhile, k_4 represents the reaction rate constant for the formation of the second catalyst.

Table 1
Kinetic parameter equations (Zaldivar et al., 1993)

Subscript i	E_{ai} (J mol ⁻¹)	Parameter p_i	k_{0i}
1	80,478.64	2.002×10^{-1}	5.36178×10^7 L mol ⁻¹ s ⁻¹
2	79,159.5	3.205×10^{-2}	2.8074×10^{10} L ² mol ⁻² s ⁻¹
3	69,974.6	-21.3754	3.9480×10^{10} L mol ⁻¹ s ⁻¹
4	76,6172.2	12706	1.4031×10^8 L mol ⁻¹ s ⁻¹

Multi-Objective Optimal Control Technique

The optimal control method executed in this study is CVP. The AMIGO2 package developed by Balsa-Canto et al. (2016) using a MATLAB environment is utilised for the CVP method. The CVP approach algorithm in AMIGO2 is constructed from Vassiliadis et al.'s (1994) research. It is based on discretising the control profiles, whereas state profiles remain in continuous form (Azmi et al., 2021). Therefore, the ODE solver first calculates the differential equation.

The original optimal control equations are then re-formulated into a finite-dimensional Nonlinear Programming problem for solution searching by the static optimiser. An appropriate gradient search with the Nonlinear Programming based algorithm is also required. The differential equations are solved at every iteration of the optimal solution searching. The inputs are frequently parameterised using a piecewise-constant (Rohman & Aziz, 2020; Azmi et al., 2020). The technique of parameterisation over finite elements (discretisation) and formation into Nonlinear Programming for CVP is depicted in Figure 1. The CVP method's standard procedure is described in Equations 12 to 15:

Problem:

$\underset{x,u(t),v(t)}{Min} \mu[d, U(t), V(t)]$	Objective function
$s. t. g[d, U(t), V(t)] \leq 0$	Constraints (Inequality)
$c[d, U(t), V(t)] = 0$	Constraints (Equality)
$\frac{dz}{dt} = F[x, U(t), V(t), t], \quad t \in [0,1]$	Process equation
$V(0) = V_0$	Initial condition (states)
$d^L \leq d \leq d^U$	Decision variables (bounds)
$U^L \leq U \leq U^U$	Control profile (bounds)
$V^L \leq V(t) \leq V^U$	State profile (bounds)

(12)

Step 1: The Lagrange Interpolating Polynomial is performed to discretise the control variables (CVs).

$$u_K(t) = \prod_{i=1}^k u_i \delta_i(t) \text{ where } \delta_i(t) = \prod_{1,i}^K \frac{(t-t_k)}{(t_i-t_k)}, \quad u_K(t_i) = u_i, \quad i = 1, \dots, K \quad (13)$$

Step 2: The discretised (CVs) shifted to the ODE model.

$$\frac{dV}{dt} = F(d, V(t), u_K(t), t) \text{ with } V(0) = V_0 \quad (14)$$

Step 3: The discretised - optimisation problem using the CVP method is represented by Equation (10).

$$\underset{x,u(t),v(t)}{Min} \mu[d, U(t), V(t)]$$

$$s. t. g[d, U(t), V(t)] \leq 0$$

$$c[d, U(t), V(t)] = 0$$

$$\begin{aligned} \frac{dV}{dt} &= F(d, V(t), u_K(t), t) \text{ with } V(0) = V_0 \\ d^L &\leq d \leq d^U \\ U^L &\leq U \leq U^U \\ V^L &\leq V(t) \leq V^U \end{aligned} \quad (15)$$

Step 4: In the updated dynamic model, the starting prediction for interval time t_i and decision variables d are substituted, which are then assessed using Runge-Kutta 4th order ODE solver.

Step 5: The hybrid strategy (HS) is utilised to compute the target and constraints in Equation 15 that are evaluated in Step 4 based on the d values. Steps 4–5 are reiterated until convergence is reached.

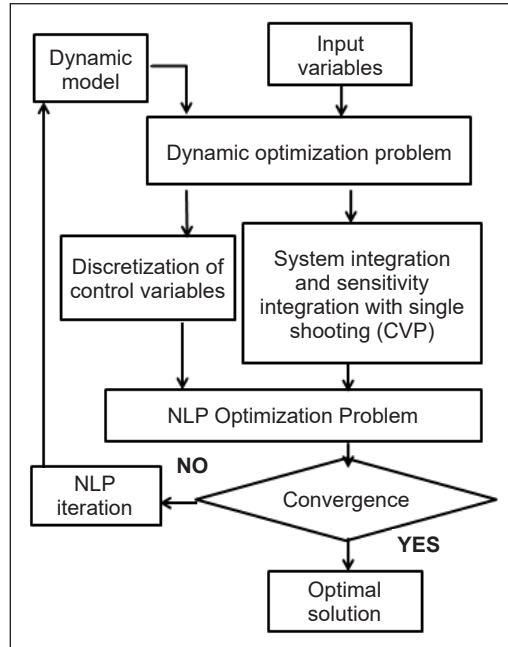


Figure 1. Optimal control method basic procedure: CVP

Hybrid Based Nonlinear Programming Solver. As a Nonlinear Programming solver, two phases of stochastic and deterministic-based optimisation are utilised. First, the stochastic-based Nonlinear Programming solver selects Differential Evolution (DE) (Storn and Price, 1997). In the meantime, sequential quadratic programming (SQP) is considered a deterministic Nonlinear Programming solver. However, it is worth noting that SQP algorithms are tended to multimodal solutions and drag to a premature solution, especially if they start further away from the optimal solution. As a result, the stochastic method, such as differential evolution (DE), is an excellent strategy to resolve the optimisation problem because it can drift away from finding local solutions while locating the optimal solution in reasonable computation time (Storn and Price, 1997). On the other hand, the DE method usually leads to subliminate solutions at a high computational cost. As there is always a counterbalance between convergence rapidity and robustness in both DE and SQP approaches, the HS is established by merging the main parts of the DE and SQP method, leveraging their complementing properties (Banga et al., 2015; Rohman et al., 2016).

The HS is the work of Banga et al. (2014). It is composed of two phases. In the first phase, the DE solver sought the near-optimal solution. When a convergence criterion (SC1) based on the rapid searching distance for each repetition succeeded, the population searching iteration is switched to the 2nd phase. In the final phase, this solution is computed as a near-optimal searching point for the DE solver. Finally, when a convergence criterion

(SC2) is met to achieve a better optimal solution, the optimiser has reached the final convergence and ends the searching process. The SC1 and SC2 convergence values of 0.02 and 10^{-6} , respectively, are determined by empirical data (Storn and Price, 1997; Banga et al., 2015; Rohman et al., 2016). Figure 2 depicts the general steps of the HS method.

Multi-Objective Optimisation (MOO) Technique. The optimum results for MOOs are an arrangement of trade-off values known as the non-dominated (ND) set (Maiti et al., 2011). A set is ND set if it is impossible to enhance one target without

loosening the other's value; the ND set is the most optimum solution for all target functions. The MOO is addressed at each repetition in this method to provide an ND set. The PF and possible counterbalance between target functions can be constructed by updating a set of discontinuous points and asserting ND points obtained from numerous runs.

The ϵ -constraint approach is one of the MOO techniques studied. There is no accumulation in the single target function in the ϵ -constraint technique; the HS optimiser solves the first target. The second target is a constraint using convergence's tolerance values ϵ . The ND points on the PF are updated by gradually changing the ϵ for multiple runs (Rohman et al., 2016). Therefore, the problem can be written as Equation 16:

$$\begin{aligned}
 & \text{Min}_{x,u(t),z(t)} \mu_1[d, U(t), V(t)] \\
 & \text{Subject to} \\
 & \mu_2[d, U(t), V(t)] \leq \epsilon \\
 & F[x, U(t), V(t), t] \in S
 \end{aligned} \tag{16}$$

The ϵ is progressively changed in multiple runs to provide the optimal points on the PF (Rohman et al., 2016). For each optimiser run, HS is utilised for the optimal solution searching.

Problem Optimisation Formulation. The decision variable is the piecewise constants of TR and FR. The catalyst, reactant, and product concentrations are regarded as state

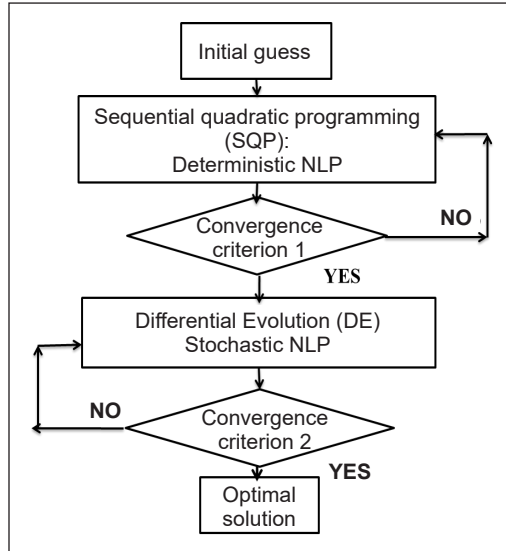


Figure 2. General steps of the HS

variables, and their values are demonstrated as process dynamics for the semi-batch course. As a simplified process model, the catalysed esterification process equations are considered. It only requires the state's differential Equations 4 to 10. This model states optimal profiles of FR and TR, which are employed to accomplish the reactor's target performance. The bounds are specified based on the TR's range capacity (303K- 343K) and pump flow rate ($0 - 5 \times 10^{-4}$ L/s), respectively. The total process time is made up of six intervals of time Δt , which are counted as free final time. As a result, the length of the interval time, Δt , is also optimised, with a range of 10min–30min.

The bi-target functions are to maximise XM while decreasing t_f . The target function is expressed to be of the form min function (to minimise). To maximise $\frac{C_{A0}V_0 - C_A V}{C_{A0}V}$, the max function is expressed as $\min - \left(\frac{C_{A0}V_0 - C_A V}{C_{A0}V} \right)$. The solution volume in the final time, 2L, served as the inequality constraint. The optimal control problem is mathematically formulated as Equation 17:

$$\begin{aligned} \min_{T(t), Fo(t)} \phi_1 &= - \left(\frac{C_{A0}V_0 - C_A V}{C_{A0}V} \right) \\ \min_{T(t), Fo(t), \Delta t} \phi_2 &= t_f \\ \text{Subject to: } Mdx/dt &= f(x(t), u(t), p, t) && \text{(model equation)} \\ 0 \leq F_0 &\leq 5 \times 10^{-4} \text{ L/s} && \\ 303\text{K} \leq T &\leq 343\text{K} && \text{(Lower and upper bounds)} \\ 10 \text{ min} \leq \Delta t &\leq 30 \text{ min} && \text{(Final inequality constraint)} \end{aligned} \quad (17)$$

RESULTS AND DISCUSSION

The Pareto Front (PF) chosen, i.e., ϵ -constraint, as shown in Figure 3, is segregated into three zones. The lower end of the PF (zone 1) is denoted by a relatively short t_f and a lower XM rate. The upper end of the PF (zone 3) is indicated by a relatively long t_f and a high XM rate. Finally, zone 2, positioned between zones 1 and 3, is designated as having a medium t_f and XM rate.

Each point of PF in Figure 3 is associated with a unique FR and TR profile. From Figures 4 to 6, ND points of A, B, and C, positioned in zones 1, 2, and 3, respectively, show a different trend of profiles. Table 2 shows the optimal control results for ND points A, B, and C, based on two reactor performances, regarded as t_f and XM.

Table 2 explains that the t_f for ND points A, B, and C is 46 min, 55 min, and 67 min, respectively. The XM for ND points A, B, and C is 0.994, 0.998, and 0.999, respectively. The variation in the conversion. i.e., 0.992 to 0.999 (Figure. 3: Pareto Front results) is significant

to be explored. The objectives obtained from PF show significant improvement of SOO results where the combination of t_f and XM obtained was 80 min, 0.999 (for maximising XM problem) and 60 min, 0.970 (for minimising t_f problem) (Rohman et al., 2021b). Furthermore, the variation in the conversion. i.e., 0.992 to 0.999 (Figure 3: Pareto Front results) is significant to be explored. It is because the profit value obtained from SOO results varied from RM/year 4.55×10^6 (maximise XM) to RM/year 5.51×10^6 (minimise t_f) (Rohman et al., 2021b); thereby, the increment of 0.001 XM with different t_f will differ profit value significantly.

TR is a decision variable that has a prominent effect on t_f and XM. The reaction rates for the reactant, product, and catalyst escalated with elevating TR (Ubrich, 2000). As a result of the disparate TR profiles, the amount of t_f and XM varies, as shown in Figures 4b, 5b, and 6b. Due to the lowest value of the optimal profile of TR acquired, point A produced the shortest XM and t_f , and vice versa for point C.

The optimal TR profiles (Figures 4b, 5b and 6b) and FR (Figures 4a, 5a and 6a) displayed a significantly different trend and complementary effect in promoting reaction rate. As the TR profile decreased in value, the FR profile equilibrated to sustain the reaction rate by raising the FR value. A higher FR of PA can induce the autocatalytic reaction,

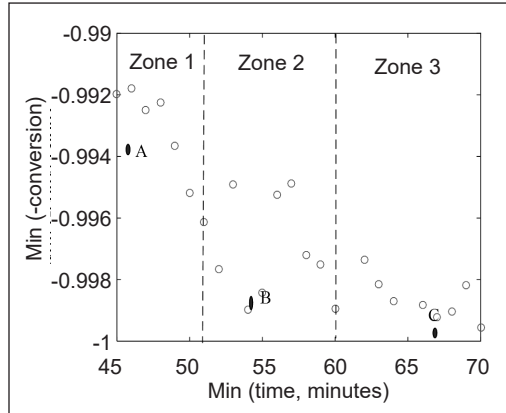
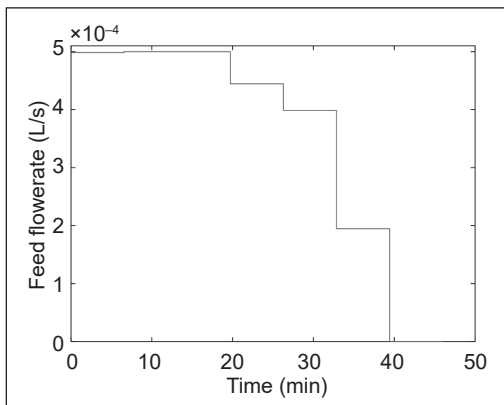


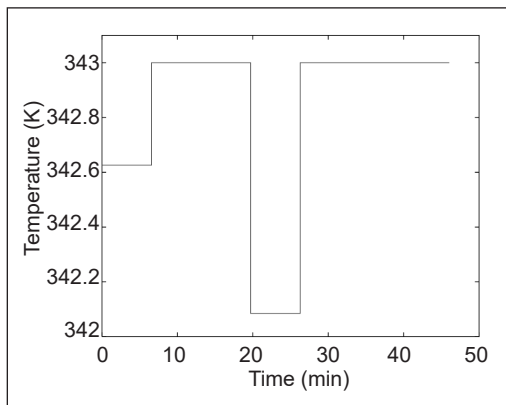
Figure 3. Pareto Front results

Table 2
Final time and conversion in points A, B, and C

Non-dominated point	A	B	C
Final time (t_f , minutes)	46	55	67
Conversion (XM)	0.994	0.998	0.999



(a)



(b)

Figure 4. Optimal trajectories in point A: (a) Feed flowrate; and (b) Temperature

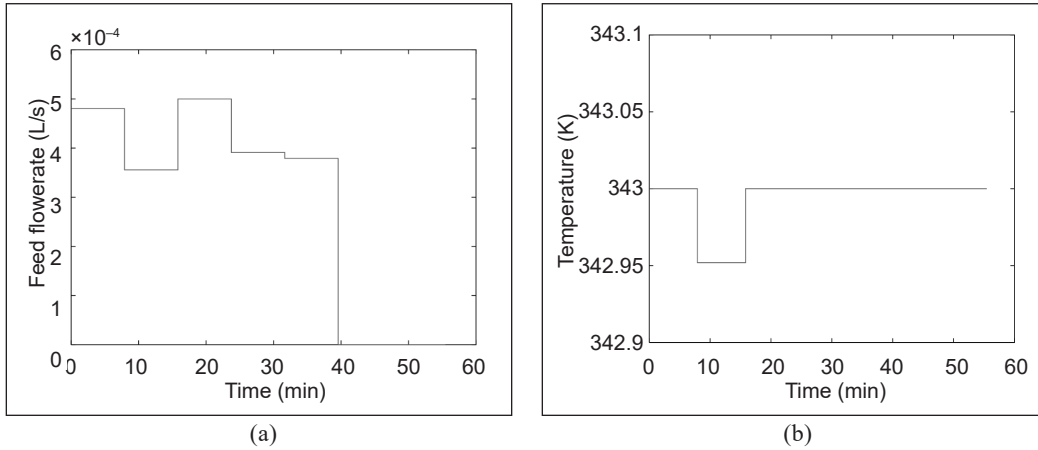


Figure 5. Optimal trajectories in point B: (a) Feed flowrate; and (b) Temperature

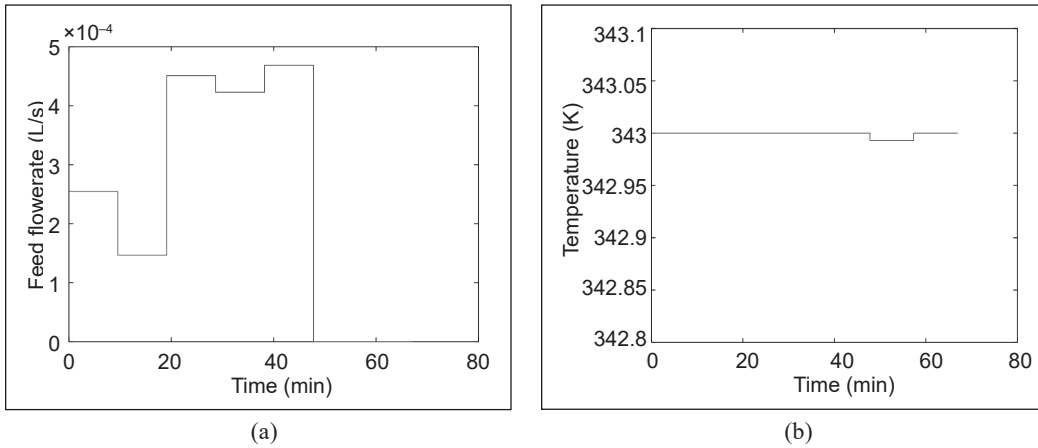


Figure 6. Optimal trajectories in point C: (a) Feed flowrate; and (b) Temperature

thereby escalating the XM rate. Furthermore, the longer the t_f , the less value of the FR. The usage of obtained PF provides the process analyst with several preferences for practical application, which refers to the trade-off between the capacity of ester production and optimal profiles extracted from PF. The increase of XM and the lessened t_f leads to profit. However, the higher TR and FR yield a rise in energy consumption and material cost, respectively. Therefore, it is found that the ND point in zone II (point B) can be selected as the trade-off of the optimal TR and FR in this study.

CONCLUSION

In a semi-batch reactor, the ester production process often has multiple performance targets, some conflicting with one another. For optimal control solver, the CVP and HS have been utilised. The ϵ -constraint has been performed to find PF solutions for the constrained

MOOC problem of minimising t_f and maximising XM. Each ND points along the PF have a variation of optimal FR and TR profiles, resulting in various t_f and XM values. The information contained within the PF enables the process analyst to examine the trade-offs between distinct target functions and to select an appropriate optimal strategy for the ester production. The critical study is that the optimal TR profile resulting from the chosen ND point becomes a pre-specified set point. Point B can be considered the most efficient of optimal TR and FR. The tracking controller then maintains the performance reactor in practice. The multi-objective optimisation study in terms of economic function can be considered a future study.

ACKNOWLEDGEMENT

This research received financial support from the College of Engineering, Universiti Teknologi MARA, Shah Alam through Synergy 2021 Grant No. 600-TNCPI 5/3/DDF (FKK) (009/2021).

REFERENCES

- Azmi, A., Sata, S. A., Rohman, F. S., & Aziz, N. (2020). Optimization studies of low-density polyethylene process: Effect of different interval numbers. *Chemical Product and Process Modeling*, 15(4), Article 20190125. <https://doi.org/10.1515/cppm-2019-0125>
- Azmi, A., Sata, S. A., Rohman, F. S., & Aziz, N. (2021). Dynamic optimization of low-density polyethylene production in tubular reactor under thermal safety constraint. *Chemical Industry and Chemical Engineering Quarterly*, 27(1), 85-97. <https://doi.org/10.2298/CICEQ190108027A>
- Balsa-Canto, E., Henriques, D., Gábor, A., & Banga, J. R. (2016). AMIGO2, a toolbox for dynamic modeling, optimization and control in systems biology. *Bioinformatics*, 32(21), 3357-3359. <https://doi.org/10.1093/bioinformatics/btw411>
- Banga, J. R., Balsa-Canto, E., Moles, C. G., & Alonso, A. A. (2005). Dynamic optimization of bioprocesses: Efficient and robust numerical strategies. *Journal of Biotechnology*, 117(4), 407-419. <https://doi.org/10.1016/j.jbiotec.2005.02.013>
- De, R., Bhartiya, S., & Shastri, Y. (2019). Multi-objective optimization of integrated biodiesel production and separation system. *Fuel*, 243, 519-532. <https://doi.org/10.1016/j.fuel.2019.01.132>
- Faust, J. M., Hamzehlou, S., Leiza, J. R., Asua, J. M., Mhamdi, A., & Mitsos, A. (2019). Dynamic optimization of a two-stage emulsion polymerization to obtain desired particle morphologies. *Chemical Engineering Journal*, 359, 1035-1045. <https://doi.org/10.1016/j.cej.2018.11.081>
- Maiti, S. K., Lantz, A. E., Bhushan, M., & Wangikar, P. P. (2011). Multi-objective optimization of glycopeptide antibiotic production in batch and fed batch processes. *Bioresource Technology*, 102(13), 6951-6958. <https://doi.org/10.1016/j.biortech.2011.03.095>
- Rohman, F. S., & Aziz, N. (2020). Dynamic multi-objective optimization of autocatalytic esterification in semi batch by using control vector parameterization (CVP) and non-dominated sorting genetic algorithm

- (NSGA-II). *IOP Conference Series: Materials Science and Engineering*, 778, Article 012081. <https://doi.org/10.1088/1757-899X/778/1/012081>
- Rohman, F. S., Sata, S. A., & Aziz, N. (2016). Online dynamic optimization strategy for handling disturbance in semi batch autocatalytic esterification process: Application of hybrid optimizer and simple re-optimization activator. *Advanced Science Letters*, 22(10), 2729-2733. <https://doi.org/10.1166/asl.2016.7021>
- Rohman, F. S., Sata, S. A., Othman, M. R., & Aziz, N. (2021a). Dynamic optimization of autocatalytic esterification in a semi-batch reactor. *Chemical Engineering & Technology*, 44(4), 648-660. <https://doi.org/10.1002/ceat.202000308>
- Rohman, F. S., Sata, S. A., Othman, M. R., & Aziz, N. (2021b). Optimizing autocatalysis with uncertainty by derivative-free estimators. *Optimal Control Applications and Methods*, 42(1), 180-194. <https://doi.org/10.1002/oca.2668>
- Storn, R., & Price, K. (1997). Differential evolution - A simple and efficient heuristic for global optimization over continuous spaces. *Journal of Global Optimization*, 11, 341-359. <https://doi.org/10.1023/A:1008202821328>
- Ubrich O. (2000). *Improving safety and productivity of isothermal semi batch reactor by modulating feed rate* (Doctoral dissertation). Swiss Federal Institute of Technology Lausanne, Switzerland.
- Vassiliadis, V. S., Sargent, R. W., & Pantelides, C. C. (1994). Solution of a class of multistage dynamic optimization problems. 1. Problems without path constraints. *Industrial & Engineering Chemistry Research*, 33(9), 2111-2122. <https://doi.org/10.1021/ie00033a014>
- Zaldivar, J. M., Hernandez, H., Molga, E., Galvan, I. M., & Panetsos, F. (1993). The use of neural networks for the identification of kinetic functions of complex reactions. In *Proceedings of the third European symposium on computer aided process engineering, ESCAPE* (Vol. 3). Oxford Press.
- Zulkeflee, S. A., Rohman, F. S., Sata, S. A., & Aziz, N. (2021). Autoregressive exogenous input modelling for lipase catalysed esterification process. *Mathematics and Computers in Simulation*, 182, 325-339. <https://doi.org/10.1016/j.matcom.2020.11.006>

